

Modulational-instability-induced supercontinuum generation with saturable nonlinear response

R. Vasantha Jayakantha Raja, K. Porsezian, and K. Nithyanandan

Department of Physics, Pondicherry University, Pondicherry-605 014, India

(Received 6 May 2010; published 21 July 2010)

We theoretically investigate the supercontinuum generation (SCG) on the basis of modulational instability (MI) in liquid-core photonic crystal fibers (LCPCF) with CS₂-filled central core. The effect of saturable nonlinearity of LCPCF on SCG in the femtosecond regime is studied using an appropriately modified nonlinear Schrödinger equation. We also compare the MI induced spectral broadening with SCG obtained by soliton fission. To analyze the quality of the pulse broadening, we study the coherence of the SC pulse numerically. It is evident from the numerical simulation that the response of the saturable nonlinearity suppresses the broadening of the pulse. We also observe that the MI induced SCG in the presence of saturable nonlinearity degrades the coherence of the SCG pulse when compared to unsaturated medium.

DOI: [10.1103/PhysRevA.82.013825](https://doi.org/10.1103/PhysRevA.82.013825)

PACS number(s): 42.65.Wi, 42.81.Dp, 42.65.Tg

I. INTRODUCTION

The supercontinuum (SC) is the generation of intense ultrafast broadband high coherent pulses spanning over a few octaves which emerge as the technology of choice for a future generation of broadband source [1,2]. With the rapid advancement in photonic crystal fiber (PCF) technology, SC gains momentum and evolves as one of the most elegant and dramatic effect in optics with a wide range of potential applications in various fields such as frequency metrology, biomedical sensors, optical coherence tomography, wavelength division multiplexing, etc. [3–7]. PCFs with a high degree of flexibility in the designing of its micro-structured cladding endowed with significantly tailorable modal properties like adjustable zero dispersion, effective mode area, and nonlinear parameter are a potential customer for generating SC [3,8]. Since the first observation of supercontinuum generation (SCG) in PCF by Ranka *et al.* [9], extensive experimental and theoretical efforts have been devoted to identify the underlying spectral broadening mechanisms. The effects of the input pulse such as pulse energy, peak power, pulse duration, and central wavelength on the SCG is the subject of high interest that has been thoroughly investigated [1,2]. Also, the nonsilica technology such as, AS₂Se₃, SF₆, TF₁₀, etc., has now emerged as the most exciting prospects in the development of PCFs [3], as they amount to increase the broadband generation. The detailed physical aspects of SCG can be interpreted by means of interplay of various nonlinear effects like self-phase modulation, Raman scattering, and four wave mixing (FWM). Among the various nonlinear phenomena, a key nonlinear process known as a soliton was proposed by Hasegawa and Tapert in [10], which arises through the balance of anomalous dispersion and self-phase modulation, plays an essential role in the SCG mechanism [10]. A complete theory of SCG by making use of soliton related effects was proposed by Husakou *et al.* [11], which has been confirmed by experiments and numerical simulations in the femtosecond regime [4]. Among the soliton related effects, two vital aspects of a high degree of importance are: the soliton frequency shift induced by Raman scattering and emission of dispersive radiation [12].

SCG, the means of generating an ultra broadband spectrum, is typically achieved by two mechanisms, namely, soliton fission and modulation instability (MI) [13]. The former leads to the generation of an ultra broadband spectrum, where

pulse breaking arises mainly due to higher-order effects of soliton-related dynamics such as higher-order linear dispersion terms and nonlinear Raman scattering. A higher order soliton with soliton order N breaks up into N constituent red shifted solitons with varying group velocities. In principle, the energy of the fundamental soliton does not change, but it emits blue-shifted nonsolitonic radiation known as dispersive radiation at a wavelength determined by phase matching condition as a result of perturbation by third- and higher-order dispersion. The distinct spectral fractions arise due to the existence of multisolitons with different frequencies resulting in a broad spectrum as a consequence of nonlinear interactions between a soliton and blue shifted continuum [12,14,15]. The physical phenomenon of soliton fission and spectral broadening of pulse in fiber have been already investigated in detail. For instance, in 1985, Dianov *et al.* [16] discovered the soliton Raman self-scattering effect. The authors reported a Raman self-pumping of the Stokes frequency spectral components of the same pulse by a sufficiently powerful (capable of producing $N = 30$ soliton) input into a single-mode quartz optical fiber and a generation of the broad soliton supercontinuum during the stimulated Raman self-scattering of $N = 30$ wave packet. In 1986, Mitschke and Mollenauer reported an increasing red shift of the center frequency of a sub-picosecond soliton pulse with increasing power in standard single-mode, polarization maintaining fiber [17]. Following the above theoretical prediction and experimental realization of broadband continua based on soliton effects, the latter part of the decade saw extensive investigation of this mechanism for broadband generation using a variety of pump laser sources and pump durations.

The latter is the MI induced SCG (MI-SCG), one of the fascinating manifestations of MI is a way of achieving an ultra broadband spectrum [18,19]. MI, an instability mechanism driven by soliton dynamics, was first proposed by Hasegawa and Brinkman in 1980 [20]. In principle, MI can be achieved by a small modulation in amplitude or phase in the presence of noise or some other perturbation. The MI can be interpreted as a FWM process phase matched through nonlinear and dispersive effects, resulting in the exponential growth of the Stokes and anti-Stokes sidebands at the expense of a two pump photon [21]. In addition to noise induced MI, it is also possible to initiate the process by feeding with a countersignal

at a frequency separation from the pump lying within the gain window. This way of achieving MI by means of a co-propagating signal was proposed by Hasegawa in 1984 [22] and verified experimentally by Tai *et al.* [23]. This mechanism is actually responsible for a controlled MI process that allows manipulation and enhancement of the SCG process. Early investigations of MI-SCG were realized through conventional fiber in the region of low dispersion regime to enhance the broadband spectrum; later the idea became effectively adopted to achieve the same in PCF. For instance, it was shown in 1983 that a continuum spectrum can be attributed by the superposition of sequential stimulated Raman scattering and FWM processes in a multimode fiber using two pump wavelengths by reducing pump power [24]. Also, in 1987, Serkin investigated the structure of the field characteristic formed in the region of maximal self-compression of N -soliton wave packet in a fiber. It was shown that the noise component of the field leads to a decay of the bound states of the solitons, to stochastic instability of the N -soliton pulse, and to the so-called soliton noise generation. He examines the possibility of an experimental realization of the decay of the output pulses from a soliton laser into ‘colored’ envelope solitons: ‘long-lived’ (in comparison with length scale of the dispersive spreading) nonlinear wave packets whose spectral center of gravity undergoes a frequency shift [25,26]. This possibility appears when an auxiliary fiber, with a chromatic-dispersion spectrum shifted to the long-wave direction, is used. This soliton compression, fragmentation, and spectral shifting are important mechanisms contributing to the long wavelength extension of SCG. Since most of the above investigations have used soliton fission for inducing SCG, in this paper, we pursue another possibility of SCG using MI.

The SCG process relies more on the optical nonlinearities associated with the picosecond and sub-picosecond scale pulses. Among the many nonlinear effects, stimulated Raman scattering and parametric FWM play major contributions in the SCG for pumping picoseconds and continuous wave in the anomalous group velocity dispersion (GVD) regime [3]. For the case of ultrashort pulses typically in the femtosecond regime, higher-order dispersion and higher-order nonlinear effects such as third-order dispersion, fourth-order dispersion, Raman effect, self-steepening, are measured to play an increasingly important role in the spectral broadening process [1,12]. The Kerr nonlinearity is considered to be the decisive agent in most of the common nonlinear phenomena such as self-phase modulation, the significant contender of many of the spectral broadening process observed in various domains. It is worth noting that Kerr nonlinearity can only predict the nonlinear response of the medium for low input power. But in reality, for the case of higher input power, higher-order nonlinear susceptibilities will inevitably come into play and eventually saturate the nonlinear response of the medium [18,21]. Thus at higher peak power Kerr nonlinearity is not solely going to predict the associated nonlinear effects, but requires a higher-order saturation effect to give a clear picture of the evolution of the SC spectrum. From our extensive literature review, in almost all the MI cases for SC, only the pure Kerr nonlinearity has been exploited. But, so far no convincing work has been reported yet about the impact of higher-order nonlinearity in the SC spectrum.

In recent years, much attention has been drawn toward liquid core photonic crystal fibers (LCPCF), due to the enhanced nonlinear effects compared to the silica core PCFs. The incorporation of liquids in the core region of PCF leads to unique optical properties such as ultra-flattened dispersion, broadband single-mode guidance, high birefringence, large nonlinearity, etc. [27–29]. Since the nonlinearity of CS₂ filled LCPCF is nearly 100 times larger than that of silica core PCF, the quintic nonlinearity manifests even at relatively lower peak power and subsequently leads to its saturation. For instance, Kong *et al.* [30] had investigated the quintic nonlinearity of the liquid CS₂, its apparent from their prediction that the quintic nonlinearity plays a vital role in the femtosecond regime. Since this quintic nonlinearity tends to saturate, one can expect a rich variety of information about the impact of saturation in the SCG mechanism and the subsequent influence on the coherence of the spectrum using LCPCF. The scenario that has not been addressed yet to our knowledge and thus seeds the motivation “what would happen to SCG if the light propagates in LCPCF with saturable nonlinear response?”

In this article, we have theoretically analyzed the mechanism of spectral broadening with the effect of saturable nonlinear response for the case of ultrashort pulses. The scalar effective index method (SEIM) has been employed to calculate the system parameter such as dispersion and nonlinearity of LCPCF. In order to investigate the MI-SCG in CS₂-filled LCPCF, we have utilized the well-known split-step Fourier method (SSFM) to solve the modified nonlinear Schrödinger equation (MNLSE). Further, considering LCPCF in an anomalous-GVD regime, we have theoretically examined the significance of a saturable nonlinear response in the MI-SCG. For better exploration, we have also performed coherence analysis and the quality of the generated spectrum is compared for both saturated and unsaturated cases in LCPCF through shot-to-shot noise perturbation in the pulse.

II. THEORETICAL MODEL

To understand the mechanisms leading to the SCG, wave propagation in a single-mode fiber with higher-order dispersion and saturable nonlinearity (SNL) may be described by the following MNLSE [18,21]:

$$\frac{\partial U}{\partial z} + \sum_{n=2}^4 \beta_n \frac{i^{n-1}}{n!} \frac{\partial^n U}{\partial t^n} - \frac{i\gamma|U|^2}{1 + \Gamma|U|^2} U = 0, \quad (1)$$

where U is the slowly varying amplitude of electrical-field envelope, β_n is the n th order of the dispersion parameter, γ is the Kerr parameter, $\Gamma = 1/P_s$ is the saturation parameter, and P_s is the saturation power. In order to study the influence of SNL on the MI-SCG for the case of the LCPCF, we consider the fiber with a cross section consisting of a triangular lattice of circular air holes in fused silica, with the pitch and hole diameter take values 1.8 μm and 1.44 μm , respectively. One of the holes is filled with the CS₂ liquid, forming the core of the fiber. The schematic diagram of LCPCF is shown in Fig. 1. The fiber parameters are evaluated using the SEIM which is a widely used numerical technique that provides a propagation constant of the guided modes in PCF [8,28], with the wavelength dependence of the refractive index of CS₂ included

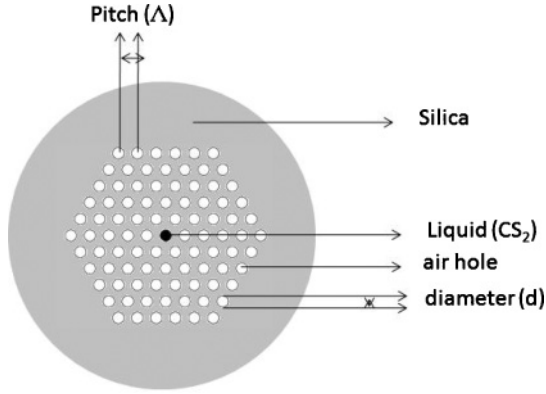


FIG. 1. Schematic diagram of the liquid-core PCF with air hole diameter d and pitch Λ . The core is filled with CS_2 and has a diameter equal to size of the air hole.

in the dispersion calculation. The wavelength dependence of the refractive index of CS_2 is given by [28] $n_{\text{CS}_2}(\lambda) = 1.580826 + 1.52389 \times 10^{-2} \times \lambda^{-2} + 4.8578 \times 10^{-4} \times \lambda^{-4} - 8.2863 \times 10^{-5} \times \lambda^{-6} + 1.4619 \times 10^{-5} \times \lambda^{-8}$, where λ is wavelength in μm . The Kerr nonlinear coefficient γ is calculated using the formula $\gamma = n_2 \omega_0 / c A_{\text{eff}}$, where c denotes the speed of light, n_2 is the nonlinear index coefficient, A_{eff} is the effective core area, ω_0 is the carrier frequency. Numerically the effective area, A_{eff} , can be calculated as in Ref. [8]. To investigate the pulse propagation in PCF, we have numerically solved Eq. (1) using SSFM with an initial envelope of the soliton at $z = 0$ given by $U(0, t) = \sqrt{P_0} \text{sech}(t)$. Numerical simulations are carried out for the input pulse at central wavelength $\lambda_0 = 1.06 \mu\text{m}$ and the pulse width of 30 fs. The fiber parameters are $\beta_2 = -0.00041 \text{ ps}^2/\text{m}$, $\beta_3 = 0.00078 \text{ ps}^3/\text{m}$, and $\beta_4 = 1.6 \times 10^{-7} \text{ ps}^4/\text{m}$ and the nonlinearity value is $\gamma = 13.75 \text{ W}^{-1}\text{m}^{-1}$ for LCPCF.

III. MI INDUCED SCG IN LCPCF

Before our investigations of MI-SCG in LCPCF, it is customary to switch off the effect of SNL for a better understanding of the MI spectrum. For instance, our discussion begins in such a way that the effect of SNL has been ignored, so as to give a comprehensible picture of MI spectrum in LCPCF. For the MI-SCG analysis, we have considered the amplitude perturbed soliton pulse with a peak power $P_0 = 400 \text{ W}$. Figure 2 depicts the MI-SCG spectrum for a propagation distance of $L = 0.8 \text{ cm}$. It is observed that the pulse gets modulated due to noise perturbation which is signified by the emergence of the spectral sidebands at the initial stage of propagation due to MI process, followed by further spectral broadening and the appearance of soliton structure on the long wavelength edge of the spectrum after 0.5 cm. This implies that MI acts directly from the beginning on the high-order soliton and leads to the generation of a Stokes and an anti-Stokes component. Because of perturbation such as higher-order dispersion and/or noise, the dynamics departs from the recurrent behavior and results in pulse breaking. The fascinating point to observe from Fig. 2 is that the Stokes components emerge at shorter distances of pulse propagation with low power, overwhelming the fact

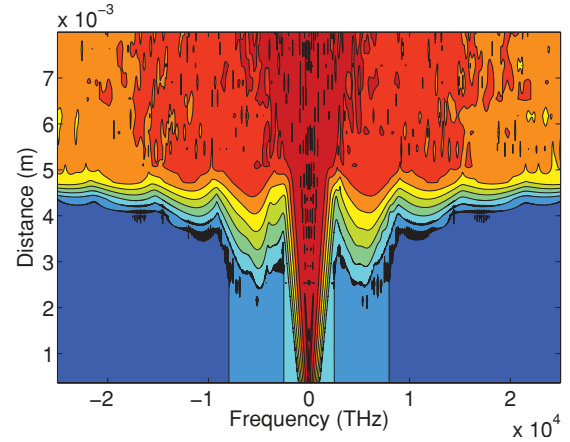


FIG. 2. (Color online) The SCG through MI of 30 fs pulse width in CS_2 filled LCPCF at $1.04 \mu\text{m}$. The fiber parameters are $\beta_2 = -0.00041 \text{ ps}^2/\text{m}$, $\beta_3 = 0.00078 \text{ ps}^3/\text{m}$, and $\beta_4 = 1.6 \times 10^{-7} \text{ ps}^4/\text{m}$ and the nonlinearity $\gamma = 13.75 \text{ W}^{-1}\text{m}^{-1}$. The propagation length $L = 0.8 \text{ cm}$.

that nonlinear and dispersion values of CS_2 filled LCPCF are very large in comparison to the ordinary solid core PCF. It is also evident from Fig. 2 that the pulse does not experience a notable asymmetric spectral broadening, which reflects the negligible role of higher-order effects in the chosen parameter region which is in agreement with Demircan *et al.* [31]. The evolution of such primary spectral side bands at the initial stage of propagation will be accompanied by the emergence of secondary sidebands after a distance $z = 0.25 \text{ cm}$. Then the subsequent spectral broadening is accomplished through FWM seeded by phase matching explosively exciting new frequencies and thus broadening the spectrum. Thus, one can achieve a broad spectrum typically SC at a relatively short distance of propagation using low input power in LCPCF rather than silica core PCF. Simultaneously, we have also analyzed the evolution of MI dynamics in time domain from Fig. 3. It is obvious from Fig. 3, as there is no phase matching between linear and nonlinear effects at the beginning, that pulse breaking is limited at the initial stage. For a relatively

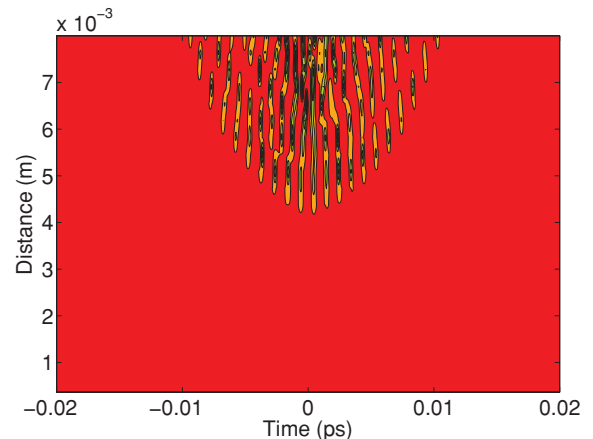


FIG. 3. (Color online) The pulse propagation through CS_2 filled LCPCF. The fiber parameters are $\beta_2 = -0.00041 \text{ ps}^2/\text{m}$, $\beta_3 = 0.00078 \text{ ps}^3/\text{m}$, and $\beta_4 = 1.6 \times 10^{-7} \text{ ps}^4/\text{m}$ and the nonlinearity $\gamma = 13.75 \text{ W}^{-1}\text{m}^{-1}$. The propagation length $L = 0.8 \text{ cm}$.

higher distance typically $z = 0.5$ cm and above, the required phase matching can be satisfactorily achieved and thus the pulse breaking starts which results in the formation of ripples in the temporal intensity profile. These ripples get spread out with further propagation thus covering the whole spectrum, resulting in the fine structure on the waveform.

IV. MI-SCG IN THE PRESENCE OF SATURABLE NONLINEARITY

Here in this context, we shift our attention toward the prime objective of the work, the effect of SNL in the MI spectrum. Considering the PCF structure as in the preceding section, we begin to explore the effect of SNL in the SC spectrum. The process of MI leading to SC can be understood by the weak perturbation of the steady state solution. The steady state solution of Eq. (1) can be written as [14]

$$U = \sqrt{P_0} \exp[i\phi(z)], \quad (2)$$

where P_0 is the input pump power and ϕ is the nonlinear phase shift which can be defined as

$$\phi(z) = \frac{\gamma P_0 z}{1 + \Gamma P_0}. \quad (3)$$

To examine the stability of the steady state solution, inserting a time-dependent weak perturbation $a(z, t)$ of frequency Ω and wave vector K , which satisfies the $a \ll P_0$ and linearizing in $a(z, t)$, one will arrive into the dispersion relation. The corresponding gain spectrum is given by

$$G(\Omega) = 2 \operatorname{Im}(K) = 4 \sqrt{\tilde{\gamma}^2 P_0^2 - \left(\tilde{\gamma} P_0 + \beta_2 \frac{\Omega^2}{2} + \beta_4 \frac{\Omega^4}{24} \right)^2} \quad (4)$$

where $\tilde{\gamma} = \gamma / (1 + \Gamma P_0)^2$. It is quite interesting to observe that, as in the case of unsaturated nonlinearity, the third-order dispersion is merely insignificant and does not play any role in the gain of the spectrum. The equation offers a rich variety of information which could be efficiently exploited in many ways.

For the case of large negative β_2 values, the higher order dispersion effects are relatively negligible. In this dispersion domain the SNL leads to a critical modulational frequency as $\Omega_c = \left[\frac{4\gamma P_0}{|\beta_2|(1+\Gamma P_0)^2} \right]^{1/2}$. In the typical operating condition of unsaturated PCF, the required phase matching to acquire MI is achieved through the compensation of second-order dispersion with Kerr nonlinearity. Quite interestingly in LCPCF, the incorporation of SNL of the medium encounters additional phase shift to achieve the phase matching. Such a condition leads to behaviors that qualitatively differ depending on the magnitude of dispersion and saturation power. Thus emphasizing the sensitivity of MI toward the saturation power and dispersion on the MI spectrum. Since the MI bandwidth increases as Γ decreases, the effect of MI can become very strong for high saturation power. In the vicinity of the near zero-dispersion regime, the fourth-order dispersion enters inevitably into play. Hence in the fourth-order dispersion dominant system, the critical modulational frequency is given by $\Omega_{opt} = \left[\frac{48\gamma P_0}{|\beta_4|(1+\Gamma P_0)^2} \right]^{1/2}$. For $\Gamma = 0$, it is noteworthy that the MI gain and critical frequencies coincide exactly with the case

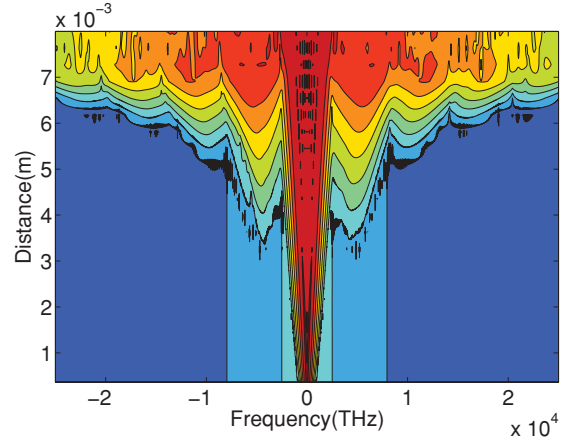


FIG. 4. (Color online) The MI-SCG with saturable nonlinearity for 30 fs of pulse width in CS_2 filled LCPCF at $1.04 \mu\text{m}$. $\beta_2 = -0.00041 \text{ ps}^2/\text{m}$, $\beta_3 = 0.00078 \text{ ps}^3/\text{m}$, and $\beta_4 = 1.6 \times 10^{-7} \text{ ps}^4/\text{m}$ and the nonlinearity $\gamma = 13.75 \text{ W}^{-1}\text{m}^{-1}$ with saturation power $P_s = 2000 \text{ W}$. The propagation length $L = 0.8 \text{ cm}$.

of unsaturated nonlinearity as discussed in Ref. [31]. Since, the prime focus of the paper is to investigate the influence of SNL, we have considered the PCF parameter with large β_2 value. Although the higher-order dispersion coefficients are momentous in PCF, the role of sixth-order dispersion is literally insignificant for MI in the given PCF structure. Hence we limit ourselves up to fourth-order dispersion. In order to investigate the dynamical behavior of the MI process with the effect of SNL, we consider the same PCF parameters as in the preceding section.

From our numerical simulation, we have obtained the results as depicted in Figs. 4 and 5 which show the effect of SNL for fixed saturation power $P_s = 2000 \text{ W}$. The inclusion of SNL, the evolution of the MI significantly changes as illustrated in Fig. 4. As per the critical frequency condition, due to the saturation effects, the phase matching can only be achieved at longer distance in comparison to that of the

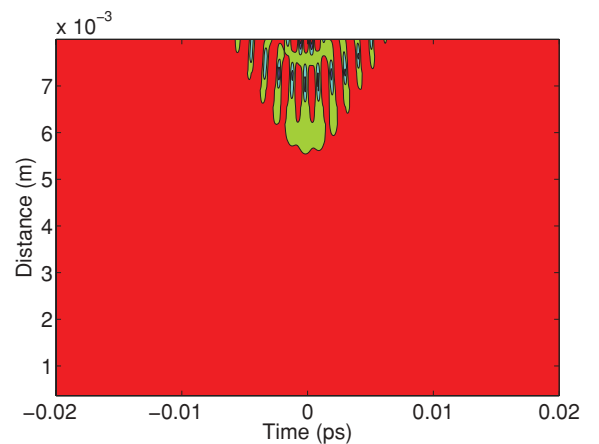


FIG. 5. (Color online) The pulse propagation through CS_2 filled LCPCF with saturable nonlinearity. The fiber parameters are $\beta_2 = -0.00041 \text{ ps}^2/\text{m}$, $\beta_3 = 0.00078 \text{ ps}^3/\text{m}$, and $\beta_4 = 1.6 \times 10^{-7} \text{ ps}^4/\text{m}$ and the nonlinearity $\gamma = 13.75 \text{ W}^{-1}\text{m}^{-1}$ with saturation power $P_s = 2000 \text{ W}$. The propagation length $L = 0.8 \text{ cm}$.

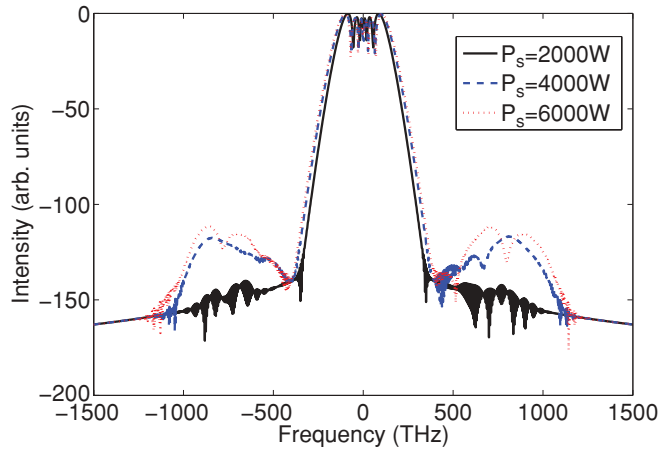


FIG. 6. (Color online) The evolution of MI phenomena for 30 fs pulse in LCPCF with different saturable powers.

unsaturated nonlinearity. Thus the SNL certainly suppresses the MI process as illustrated in Fig. 4. Hence, the spectral broadening can only be obtained at longer distance when compared to unsaturated fiber. The corresponding dynamics of pulse breaking in time domain is portrayed in Fig. 5. Since the phase matching between linear and nonlinear effects is influenced by the SNL, the pulse breaking can only be achieved at comparatively longer distance than the unsaturated LCPCF. For better insight into the picture of MI-SCG, we have investigated the evolution of MI for various saturation power as in Fig. 6. In the operating conditions of saturated nonlinearity, the optical modulational frequency not only varies with the input power of pulse but also saturation power as illustrated in Fig. 6. It is observed that the evolution of MI in LCPCF is certainly suppressed by decreasing saturation power, which means that while increasing the SNL the MI-SCG gets suppressed. Figure 7 depicts spectral evolution of MI-SCG in the presence of SNL with different saturation power. It is obvious from Fig. 7 that the saturable LCPCF also shows flat spectrum, where the spectral density at the peak varies merely less than 10 dB over a bandwidth 800–1500 nm. It is also

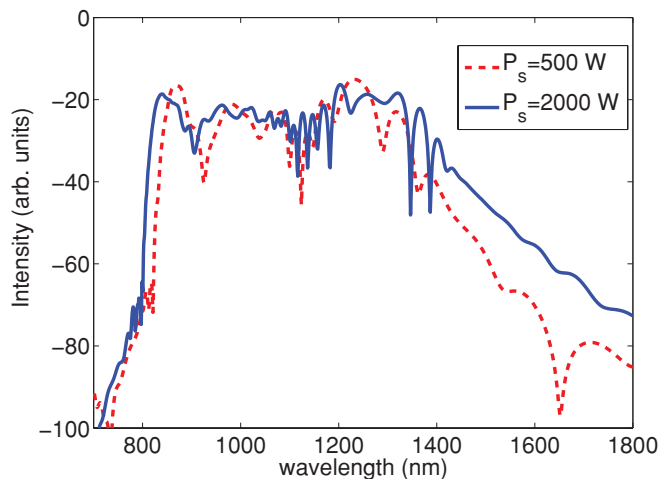


FIG. 7. (Color online) SCG using MI for for different saturation power.

observed that the spectral broadening quantitatively gets suppressed with a decrease in the saturation power.

V. QUALITY ANALYSIS OF MI-SCG IN LCPCF

We now turn our attention to explore the quality of the pulse, which is considered to be the essence of all broadband generations. It is an interesting point to note that the quality in this context has been customized to mean the coherence of the obtained SCG spectrum. Although we limit ourselves to investigate the MI-SCG, there exists another well known mechanism known to our knowledge as the soliton fission, which has been recognized as the ultimate choice of achieving a supreme quality broadband spectrum with the highest degree of spectral purity. For a better understanding of the coherence and the associated spectral purity of the SCG, we have numerically investigated SCG through soliton fission with the same parameter as the preceding section with the inclusion of SNL, as illustrated in Fig. 8. From Figs. 7 and 8 it is observed that the spectral broadening in the presence of SNL in LCPCF is almost similar in both cases. Further, for better insight into the quality of the SCG spectrum, we have studied the shot-to-shot coherence analysis for the generated SC to compare the quality of the pulse. The degree of coherence of the SC which is the measure of spectral phase stability is qualitatively calculated by the following expression as in Ref. [32]:

$$|g_{12}^{(1)}(\lambda)| = \left| \frac{\langle E_1^*(\lambda)E_2(\lambda) \rangle}{[\langle |E_1(\lambda)|^2 \rangle \langle |E_2(\lambda)|^2 \rangle]^{1/2}} \right|. \quad (5)$$

Here, the ensemble average over independently generated SC pairs $[E_1(\lambda), E_2(\lambda)]$ is represented by the angle brackets. We applied the ensemble average of SC pairs obtained from MI with different random quantum noise. The coherence analysis of the SCG spectrum obtained through both mechanisms results in rich class of information about the quality means of generating SCG. From our detailed numerical analysis, we figure out the following results which govern the entire coherence cum quality of the SCG obtained through two well-known mechanisms, namely MI and soliton fission, with and without SNL.

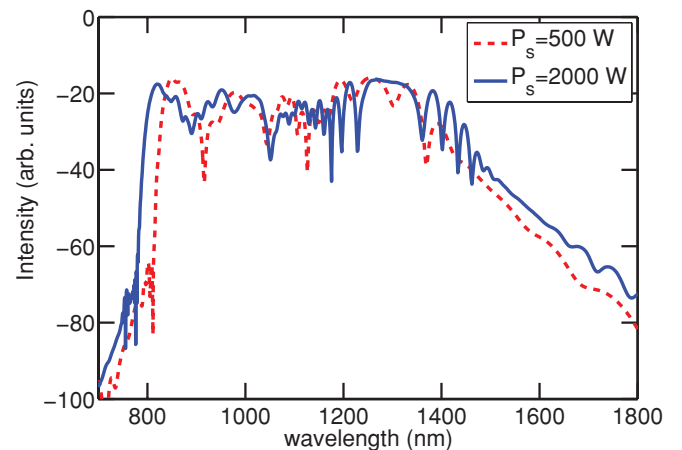


FIG. 8. (Color online) SCG using soliton fission for different saturation power

The coherence of the spectrum in the absence of SNL, such as the one indicated in Fig. 8 for the case of soliton fission induced SCG, is 0.93, and inclusion of SNL is 0.91. It is also observed that the coherence of MI-SCG in LCPCF with the effect of saturable nonlinear response is only 0.47, while the unsaturable case leads to 0.5. Since the MI process is highly sensitive to input noise, the obtained SC pulses are severely affected by spectral phase instabilities during the propagation. Hence, the coherence of the MI-SCG degrades significantly in comparison to SCG generated by soliton fission. Also, we have observed through numerical simulation that the coherence still lowers with the incorporation of saturable response medium.

VI. CONCLUSION

In conclusion, we have investigated the dynamics of SC pulse in CS₂ filled LCPCF based on MNLSE which includes the combined effects of Kerr-type nonlinearity and SNL in the femtosecond regime. We have organized our investigation of MI-SCG phenomenon by first considering the influence of LCPCF in the MI mechanism by ignoring the saturable response of the medium. We have compared our results with silica core PCF and confirmed that MI-SCG in LCPCF can be

achieved at relatively short distance and at low input power. Then the subsequent investigation proceeds in such a way to explore exclusively the impact of SNL in the MI spectrum with proper theoretical prediction. It is evident from our numerical simulation that the SNL suppresses the spectral broadening and the associated pulse breaking to achieve SCG. Also, we have analyzed MI-SCG for different saturation power, the obtained results show that SCG qualitatively gets suppressed with an increase in the saturation power. To examine the quality of the obtained MI-SCG, we have performed shot-to-shot noise coherence analysis and compared our results with the SCG through soliton fission. Finally, we have arrived at a conclusion that the coherence of the broad pulse in the presence of SNL is low in comparison to the unsaturated PCF.

ACKNOWLEDGMENTS

K.P. thanks DST-DFG, DST, DAE-BRNS, CSIR, and UGC, Government of India, for the financial support through major projects. The authors thank Dr. Anton Husakou, Max Born Institute for Nonlinear Optics and Short Pulse Spectroscopy, Berlin, Germany for his useful discussion.

-
- [1] J. M. Dudley, Goëry Genty, and Stéphane Coen, *Rev. Mod. Phys.* **78**, 1135 (2006).
- [2] A. M. Zheltikov, *Phys. Usp.* **49**, 605 (2006).
- [3] *Optical Fiber Supercontinuum Generation*, 1st ed., edited by J. M. Dudley and J. R. Taylor (Cambridge University Press, Cambridge, 2010).
- [4] J. Herrmann, U. Griebner, N. Zhavoronkov, A. Husakou, D. Nickel, J. C. Knight, W. J. Wadsworth, P. St. J. Russell, and G. Korn, *Phys. Rev. Lett.* **88**, 173901 (2002).
- [5] J. M. Dudley, L. Provino, N. Grossard, H. Maillotte, R. S. Windeler, B. J. Eggleton, and S. Coen, *J. Opt. Soc. Am. B* **19**, 765 (2002).
- [6] R. Holzwarth, Th. Udem, T. W. Hansch, J. C. Knight, W. J. Wadsworth, and P. S. J. Russell, *Phys. Rev. Lett.* **85**, 2264 (2000).
- [7] J. Hartl, X. D. Li, C. Chudoba, R. K. Ghanta, T. H. Ko, J. G. Fujimoto, J. K. Ranka, and P. S. J. Russell, *Opt. Lett.* **26**, 608 (2001).
- [8] R. Vasantha Jayakantha Raja and K. Porsezian, *Phot. Nanostruct.* **5**, 171 (2007).
- [9] J. K. Ranka, R. S. Windeler, and A. J. Stentz, *Opt. Lett.* **25**, 25 (2000).
- [10] A. Hasegawa and F. Tappert, *Appl. Phys. Lett.* **23**, 142 (1973).
- [11] A. V. Husakou and J. Herrmann, *Phys. Rev. Lett.* **87**, 203901 (2001).
- [12] D. V. Skryabin and A. V. Gorbach, *Rev. Mod. Phys.* **82**, 1287 (2010).
- [13] S. Coen, A. Chau, R. Leonardt, J. Harvey, J. C. Knight, W. J. Wadsworth, and P. S. J. Russell, *J. Opt. Soc. Am. B* **19**, 753 (2002).
- [14] N. I. Nikolov, T. Sørensen, O. Bang, and A. Bjarklev, *J. Opt. Soc. Am. B* **20**, 2329 (2003).
- [15] A. V. Husakou and J. Herrmann, *J. Opt. Soc. Am. B* **19**, 2171 (2002).
- [16] E. M. Dianov, A. Y. Karasik, P. V. Mamyshev, A. M. Prokhorov, V. N. Serkin, M. F. Stelmakh, and A. A. Fomichev, *JETP Lett.* **41**, 294 (1985).
- [17] F. M. Mitschke and L. F. Mollenauer, *Opt. Lett.* **11**, 659 (1986).
- [18] J. Miguel Hickmann, S. B. Cavalcanti, N. M. Borges, E. A. Gouveia, and A. S. Gouveia-Neto, *Opt. Lett.* **18**, 182 (1993).
- [19] A. Demircan and U. Bandelow, *Opt. Commun.* **244**, 181 (2005).
- [20] A. Hasegawa and W. F. Brinkman, *IEEE J. Quant. Electron.* **16**, 694 (1980).
- [21] P. Tchofo Dinda and K. Porsezian, *J. Opt. Soc. Am. B* **27**, 1143 (2010).
- [22] A. Hasegawa, *Opt. Lett.* **9**, 288 (1984).
- [23] K. Tai, A. Hasegawa, and A. Tomita, *Phys. Rev. Lett.* **56**, 135 (1986).
- [24] M. Nakazawa and M. Tokuda, *Jpn. J. Appl. Phys., Part 2* **22**, 239 (1983).
- [25] V. N. Serkin, "Extremal compression of optical wave packets in fiber light guides", Translated Source: Soviet Physics - Lebedev Institute Reports (USA), No. 6, 1987, pp. 44–48.
- [26] V. N. Serkin, "Colored envelope solitons in optical fibers", Translated Source: Soviet Technical Physics Letters (USA), Vol. 13, No. 7, July 1987, pp. 320–321.
- [27] H. Zhang, S. Chang, J. Yuan, and D. Huang, *Optik* **121**, 783 (2010).
- [28] R. Zhang, J. Teipel, and H. Giessen, *Opt. Express* **14**, 6800 (2006).
- [29] Y. Sato, R. Morita, and M. Yamashita, *Jpn. J. Appl. Phys.* **36**, 6768 (1997).
- [30] De Gui Kong, Qing Chang, Hong'An Ye, Ya Chen Gao, Yu Xiao Wang, Xue Ru Zhang, Kun Yang, Wen Zhi Wu, and Ying Lin Song, *J. Phys. B: At. Mol. Opt. Phys.* **42**, 065401 (2009).
- [31] A. Demircan and U. Bandelow, *Appl. Phys. B* **86**, 31 (2007).
- [32] J. M. Dudley and S. Coen, *Opt. Lett.* **27**, 1180 (2002).